Hindawi Publishing Corporation
Journal of Sensors
Volume 2015, Article ID 387641, 7 pages
http://dx.doi.org/10.1155/2015/387641

Research Article

Significance of the Nanograin Size on the H_2S-Sensing Ability of CuO-SnO_2 Composite Nanofibers

Akash Katoch, Jae-Hun Kim, and Sang Sub Kim

Department of Materials Science and Engineering, Inha University, Incheon 402-751, Republic of Korea

Correspondence should be addressed to Sang Sub Kim; sangsub@inha.ac.kr

Received 27 December 2014; Accepted 14 February 2015

Academic Editor: Kourosh Kalantar-Zadeh

CuO-SnO_2 composite nanofibers with various nanograin sizes were synthesized for investigating their sensing properties with respect to H_2S gas. The nanograin size in the CuO-SnO_2 composite nanofibers was controlled by changing the thermal treatment duration under isothermal conditions. The nanograin size was found to be critical for the sensing ability of the composite nanofibers. The CuO-SnO_2 composite nanofibers comprised of small-sized nanograins were more sensitive to H_2S than those with larger-sized nanograins. The superior sensing properties of the CuO-SnO_2 composite nanofibers with the smaller nanograins were attributed to the formation of the larger number of *p*-CuO-*n*-SnO_2 junctions and their transformation to *metallic*-CuS-*n*-SnO_2 contacts upon exposure to H_2S gas. The results suggest that smaller nanograins are conducive to obtaining superior H_2S-sensing properties in CuO-SnO_2 composite nanofibers.

1. Introduction

The air quality in industrial sectors situated in urban areas, such as power plants, is of major concern. Gases, such as CO, H_2S, and NO_x, have been identified as highly toxic air pollutants. Among them, H_2S is highly flammable and hazardous to human health even at very low concentrations (<10 ppm) [1].

Semiconductor metal oxides, such as SnO_2, ZnO, NiO, CuO, TiO_2, and WO_3, have potential applications for the detection of hazardous gaseous species. Among them, *p*-type CuO is highly sensitive and selective towards H_2S [2]. *p*-type CuO transforms to *metallic*-CuS in the presence of H_2S and recovers its *p*-type CuO characteristics in air. This property of CuO has been used successfully by means of *p*-CuO-*n*-semiconductor heterostructures [2–8]. Among them, the CuO-SnO_2 composite materials are recognized as the best material system for the detection of H_2S gas [4, 6].

A range of CuO-SnO_2 composite materials systems, such as CuO-SnO_2 composite thin films [9], CuO-functionalized SnO_2 nanowires [6], and CuO-SnO_2 composite nanofibers [10], were used successfully for the detection of H_2S gas. In particular, composite nanofibers are more promising because they have the potential to manipulate the number of *p-n* junctions between CuO and SnO_2 nanograins. According to earlier studies [11, 12], the number of *p-n* junctions greatly influences the sensing ability of CuO-SnO_2 composite nanofibers. The maximum number of *p-n* junctions was essential for obtaining superior H_2S-sensing properties. On the other hand, nanograins of different sizes have also been found to affect the sensing ability of metal oxide nanofibers [13–19]. The size of the nanograins can be changed by heating at different temperatures or different time intervals under isothermal conditions.

In this study, CuO-SnO_2 composite nanofibers were synthesized and their gas sensing ability was investigated particularly in terms of the nanograin size. For this, the CuO-SnO_2 composite nanofibers were heat treated at different temperatures under isothermal conditions. The results suggest that the nanograin size has a significant effect on the H_2S-sensing ability of CuO-SnO_2 composite nanofibers, demonstrating the optimization of the nanograin size is one of key parameters to obtain the best H_2S sensing performance.

2. Experimental

The CuO-SnO_2 composite nanofibers were synthesized by an electrospinning process. The composition of the prepared

electrospinning solution is as follows: **x**CuO-(1 − **x**)SnO_2, where **x** = 0.5. The precursor materials, tin (II) chloride dehydrate ($SnCl_2{\cdot}2H_2O$, Sigma-Aldrich Corp.), copper chloride dihydrate ($CuCl_2{\cdot}2H_2O$, Junsei Chemical Co. Ltd.), and solvents N, N-dimethylformamide anhydrous (DMF, Sigma-Aldrich Corp.), ethanol (Sigma-Aldrich Corp.), and polyvinyl acetate (PVAc, Sigma-Aldrich Corp.) polymer were used to synthesize the composite nanofibers. The following gives a brief summary of the procedure for the synthesis of the CuO-SnO_2 composite nanofibers. First, a mixed DMF and ethanol solution was prepared and the PVAc polymer was added to enhance the viscosity of the prepared solution. Proper amounts of the $SnCl_2$ and $CuCl_2$ precursor materials were added to the prepared solution and stirred at room temperature for 6 h. The prepared electrospinning solution was poured into a glass syringe equipped with a 21-gauge stainless steel needle with an inner diameter of 0.51 mm. The flow rate, applied voltage, and needle to collector distance were 0.05 mL/h, 15 kV, and 20 cm, respectively. The as-spun fibers were deposited over SiO_2 (250 nm) grown Si substrates. The as-spun fibers were then calcined at 600°C at a heating rate of 10°C/min in air for different time intervals from 0.5 to 48 h. The heat treatment led to the decomposition of the polymers and precursors in the as-spun fibers and transforms them to the required oxide phase. Finally, the individual nanofibers assembled with nanosized grains were prepared.

Thermogravimetric-differential thermal analysis (TGA-DTA, STA 409 PC, Netzsch) of the prepared as-spun nanofibers was performed to determine the appropriate calcination temperature. The microstructure and phase of the prepared nanofibers were characterized by field emission scanning electron microscopy (FE-SEM, Hitachi S-4200) and X-ray diffraction (XRD, Philips X'pert MRD diffractometer).

For the sensing measurements, a bilayer electrode consisting of a 50/200 nm thick Ti/Au layer was deposited by sputtering with an interdigital electrode mask. Figure 1(a) shows a schematic diagram of the fabrication process of the CuO-SnO_2 composite nanofiber sensors. The gas sensing performance of the CuO-ZnO composite nanofibers was tested for H_2S. The sensing measurements were performed using a gas sensing system. The H_2S gas concentrations were controlled by maintaining the mixing ratio of the dry air-balanced target gas and dry air through accurate mass flow controllers. The configuration and design of the sensing system are reported elsewhere [11, 12]. The optimal measurement temperature was found to be 300°C after a series of preliminary experiments reported in the previous work [11]. The gas response, R, was evaluated from the ratio, R_a/R_g, where R_a is the resistance in the absence of H_2S and R_g is the resistance measured in the presence of H_2S.

3. Results and Discussion

Figures 1(b) and 1(c) show FE-SEM images of the as-spun nanofibers, which were composed of mixture of PVAc, copper chloride, and tin chloride with solvents. The as-spun nanofibers were distributed uniformly over the SiO_2 grown Si substrates. TGA of the as-spun nanofibers was carried out to determine the temperature at which the solvent and organic components decomposed completely. As shown in Figure 1(e), marginal weight loss occurred up to 200°C, which was attributed to the evaporation of a small amount of solvent in the as-spun nanofibers. On the other hand, the sharp weight loss at above 200°C was assigned to the degradation of the polymer chains in PVAc. The decomposition of the PVAc polymer continued up to 600°C. No further weight loss was observed above 600°C. This suggests that the calcination temperature of 600°C is needed to remove the polymer content and transform the copper chloride and tin chloride to their corresponding CuO and SnO_2 phases, respectively. TGA confirmed that the optimal calcination temperature was 600°C. Figure 1(d) shows a typical FE-SEM image of the CuO-SnO_2 composite nanofibers obtained after calcination at 600°C. The composite nanofibers were distributed randomly and uniformly over the substrate.

Figures 2(a), 2(b), and 2(c) show high magnification FE-SEM images of CuO-SnO_2 nanofibers obtained after calcination at 600°C for 0.5, 12, and 48 h, respectively. They clearly showed that all the nanofibers were composed of nanosized grains and their size changed as a function of the calcination time under the isothermal condition. The insets show the corresponding low-magnification FE-SEM images, revealing the overall features of the nanofibers. Figure 2(d) shows the summarized nanograin size as a function of the calcination time under the isothermal condition. As is evident, the nanograin size increases with increasing calcination time. The grain growth is a thermally activated process, occurring at the expense of smaller nanograins. By this grain growth phenomenon, a longer calcination time led to the generation of larger nanograins. Earlier investigations [12–14] suggest that the activation energy required for the growth of nanograins is about one order of magnitude smaller than the bulk counterparts and the growth mechanism mainly involves lattice and/or surface diffusion.

Figure 3 shows the XRD pattern of the CuO-SnO_2 composite nanofibers calcined at 600°C for 48 h. The peaks match well with the SnO_2 and CuO phases (JCPDS: 880287 for SnO_2 and JCPDS: 895899 for CuO), demonstrating the creation of CuO-SnO_2 composite material.

To examine the effects of the nanograin size on the H_2S-sensing ability of the CuO-SnO_2 composite nanofibers, the fabricated sensors were tested for 1 and 10 ppm H_2S at 300°C. Figure 4 presents the typical resistance curves of the CuO-SnO_2 nanofibers sensors with various nanograin sizes. All sensors clearly detect H_2S gas. The resistance of the sensors decreases upon the supply of H_2S and increases upon its stoppage. The response of the sensors decreases sharply with increasing nanograin size (see Figure 5(a)). The CuO-SnO_2 composite nanofibers with the smallest nanograins were the most sensitive among all the sensors. In addition, the response of the CuO-SnO_2 composite nanofibers for 10 ppm H_2S is summarized as a function of the grain size in Figure 5(b). This suggests that the composite nanofibers should be prepared with smaller nanograins; that is, the response improves with decreasing nanograin size. It is of note that the sensors fabricated in this study were stable for longer than six months and showed a negligible variance with respect to samples.

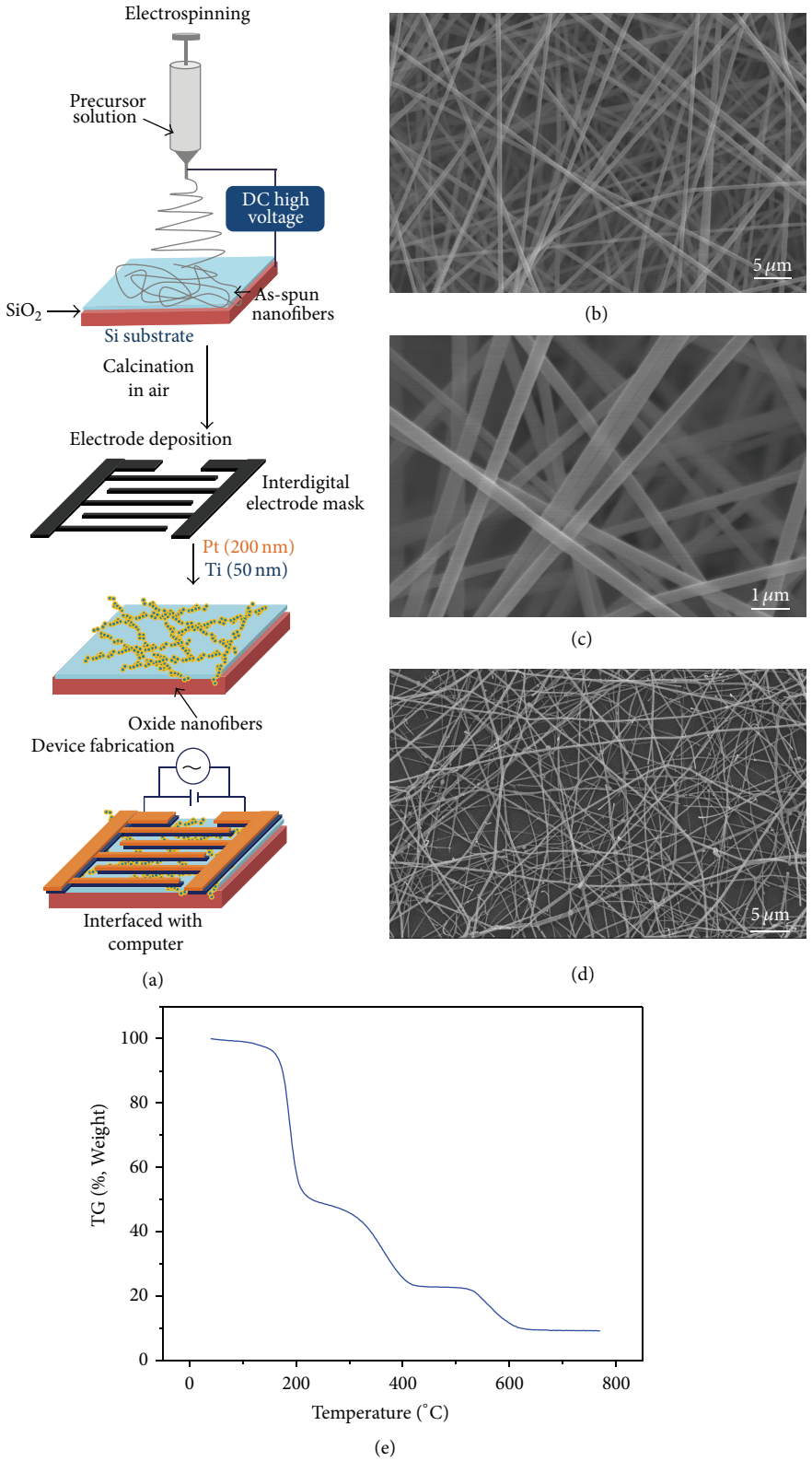

Figure 1: (a) Schematic diagram of the synthesis of CuO-SnO_2 composite nanofibers. Typical FE-SEM images of (b), (c) as-spun and (d) CuO-SnO_2 composite nanofibers synthesized by an electrospinning method. (d) Thermal profile obtained from TGA for the as-spun fibers.

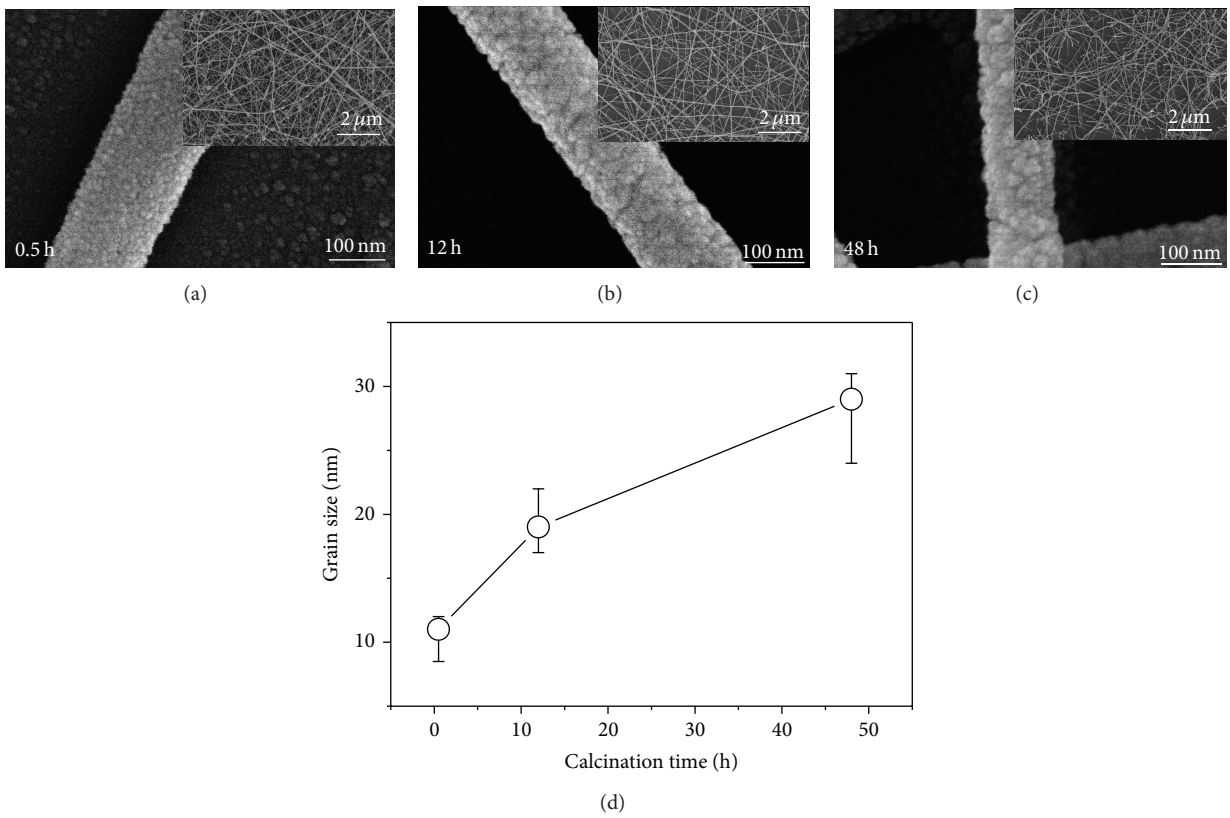

Figure 2: FE-SEM images of CuO-SnO_2 composite nanofibers calcined at 600°C for (a) 0.5, (b) 12, and (c) 48 h. (d) Summary of the grain size as a function of the calcination time.

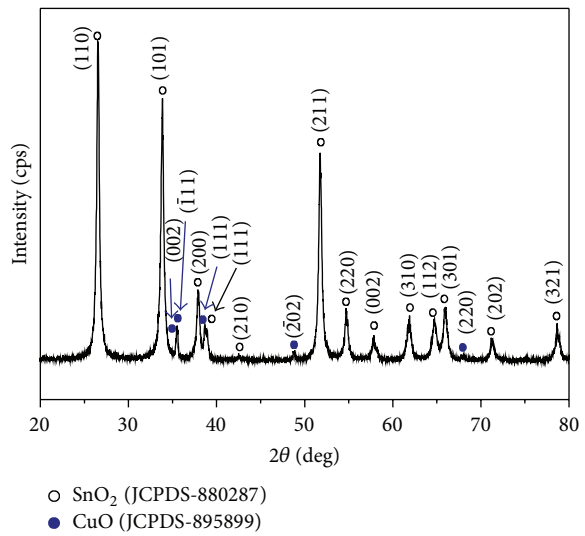

Figure 3: XRD patterns of the CuO-SnO_2 composite nanofibers calcined at 600°C for 48 h.

In the current work, the CuO-SnO_2 composite nanofibers with the nanograin size 11 nm showed the response ~25799, but the same composite nanofibers with the nanograin size 29 nm showed the response ~4399 for 10 ppm of H_2S. With the same composition but different grain sizes, there is very much difference in H_2S response, indicating the grain size is one of key parameters. Previously, the effect of composition in CuO-SnO_2 nanofibers was thoroughly investigated by some of the authors [12]. It has been found that the response was the highest at 0.5CuO-0.5SnO_2 composition. In this regard, the composition is also an important parameter. In addition, the surface structure can also influence the sensing properties

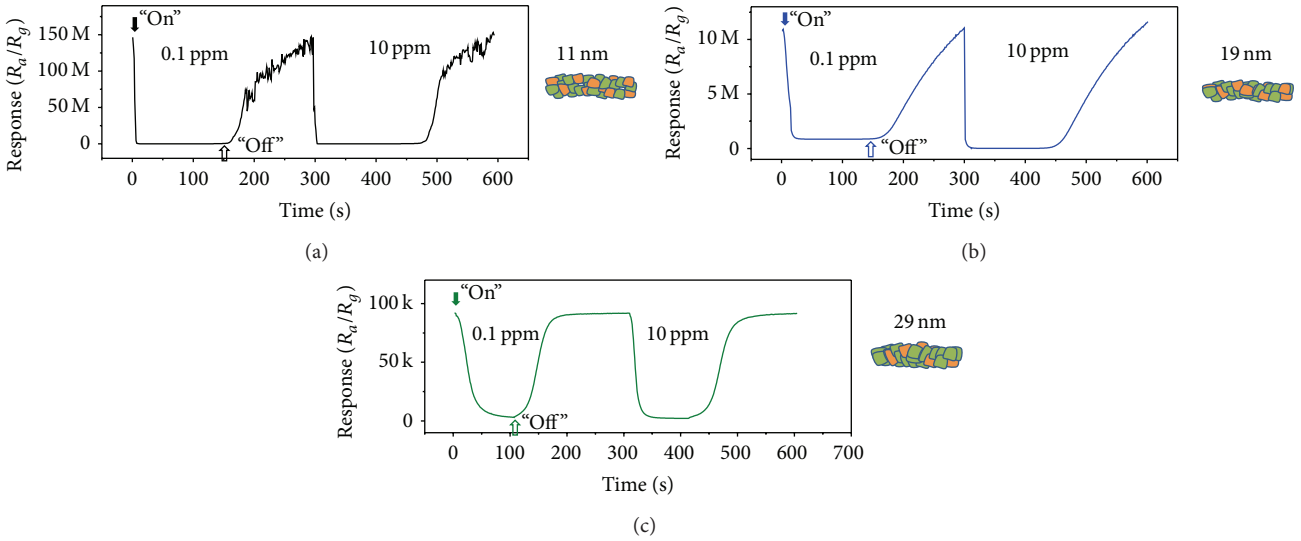

FIGURE 4: (a) Dynamic gas response curves of the CuO-SnO_2 composite nanofibers with nanograins of different sizes.

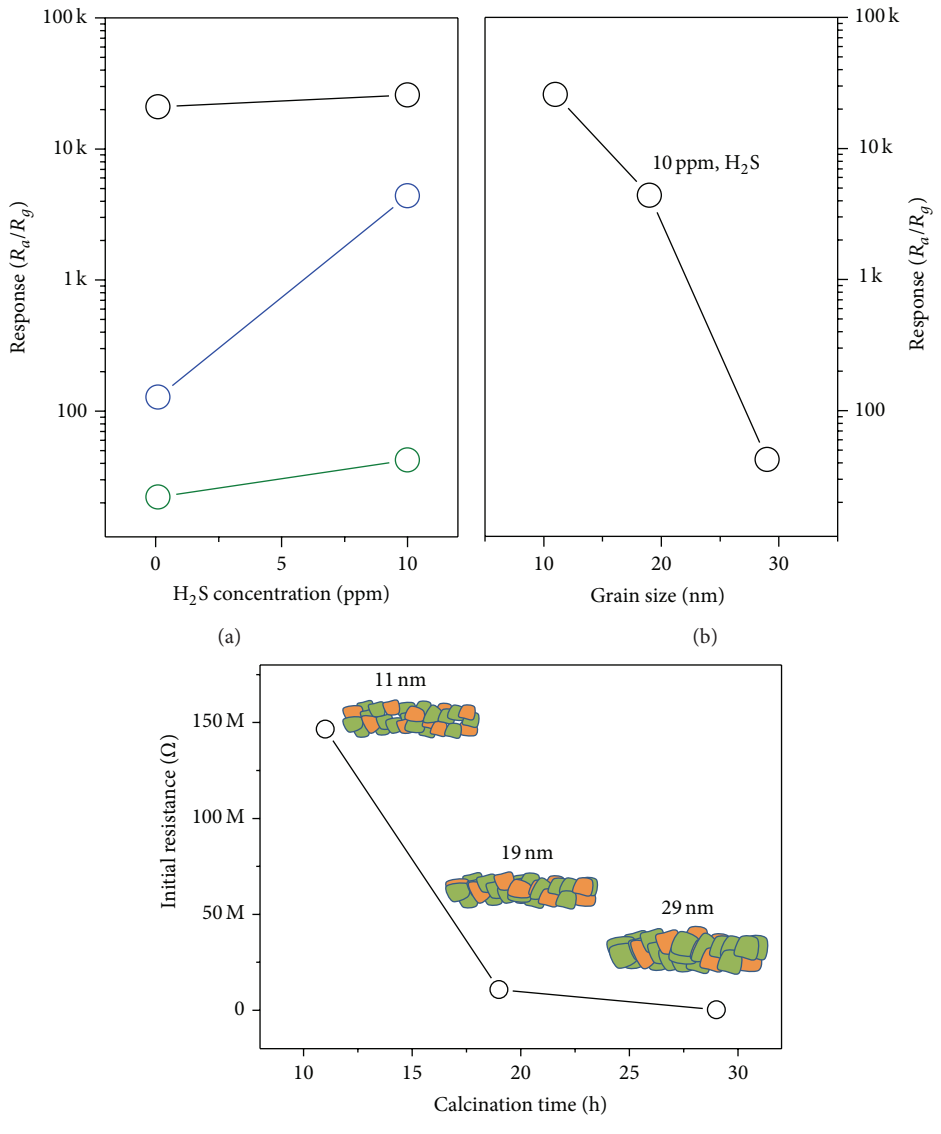

FIGURE 5: (a) Gas responses of CuO-SnO_2 composite nanofibers with nanograins of different sizes to 1 and 10 ppm H_2S gas. (b) Gas responses to 10 ppm H_2S and (c) sensor resistances of CuO-SnO_2 composite nanofibers calcined for different durations.

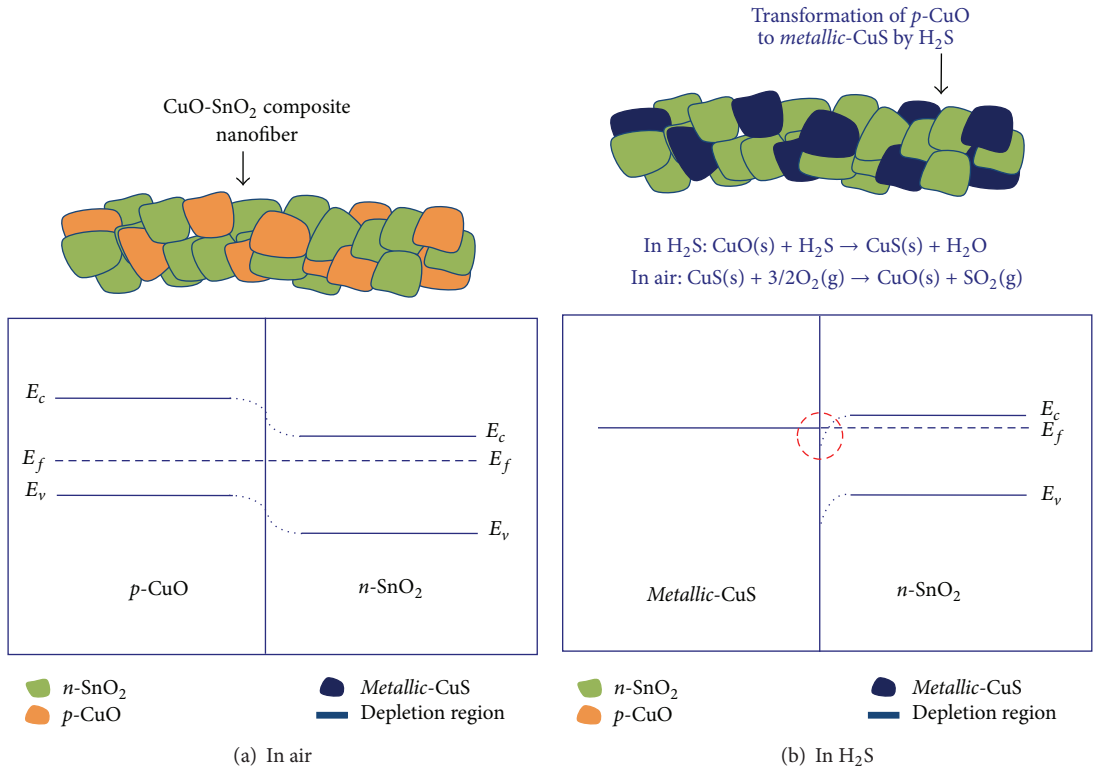

FIGURE 6: Schematic diagrams of the H_2S-sensing mechanism operated in the CuO-SnO_2 composite nanofibers.

and further investigations are required to clarify this. The response behavior of the CuO-SnO_2 composite nanofibers as a function of the nanograin size can be understood based on the formation of a number of *p-n* junctions among the neighboring CuO and SnO_2 nanograins. Previous transmission electron microscopy investigations of CuO-SnO_2 composite nanofibers confirmed that the individual CuO-SnO_2 composite nanofiber was comprised of CuO and SnO_2 nanograins [11]. Figure 5(c) summarizes the initial resistance of the CuO-SnO_2 composite nanofibers with respect to their grain size. The resistance of composite nanofibers decreases with increasing nanograin size. This suggests that the composite nanofibers with small-sized nanograins are likely to contain a large number of *p-n* junctions. Initially, the transfer of holes and electrons occurs between the CuO and SnO_2 nanograins and establishes a state of equilibrium. This results in band bending at the conduction band edge of the CuO and SnO_2 and forms a highly depleted region at the interface, which restricts the flow of electrons. The charge carriers will encounter a series of resistive *p-n* junctions in the composite nanofibers and increase the overall resistance. The CuO-SnO_2 composite nanofibers with smaller nanograins will have a larger number of *p-n* junctions, resulting in a larger resistance compared to the nanofibers composed of larger nanograins. These resistive *p-n* junctions contribute towards resistance modulation in the composite nanofibers during the absorption and desorption of gas molecules. The sensing mechanism that operates in the CuO-SnO_2 composite nanofibers is described as follows. When CuO-SnO_2 composite nanofibers are exposed to H_2S, the *p*-CuO is likely to transform to a *metallic*-CuS phase. The transformation of *p*-CuO to *metallic*-CuS is well described in the literature [2]. The transformation occurs according to the following reaction between CuO and H_2S molecules: $CuO(s) + H_2S(g) \rightarrow CuS(s) + H_2O(g)$. This leads to the destruction of the resistive *p*-CuO-*n*-SnO_2 junctions to *metallic*-CuS-*n*-SnO_2 contact and facilitates the flow of electrons from *metallic*-CuS to *n*-SnO_2. The whole phenomenon leads to a dramatic decrease in the resistance of the composite nanofibers. Upon the stoppage of the H_2S supply, the air molecules again adsorb on the *metallic*-CuS and transform it back to a *p*-CuO phase by the following reaction: $CuS(s) + 3/2O_2(g) \rightarrow CuO(s) + SO_2(g)$. In this way, it acquires its original *p-n* band configuration. Figure 6 shows a schematic diagram of the sensing mechanism.

According to Figure 5(b), the response of the CuO-SnO_2 composite nanofibers decreases sharply with increasing nanograin size. Based on the above discussion, the composite nanofibers with small nanograins consist of a large number of *p-n* junctions, which results in a larger change in resistance during the adsorption and desorption of H_2S molecules. This shows that composite nanofibers comprised of small-sizes nanograins are needed to obtain superior sensing properties.

4. Conclusion

This study examined the effects of the nanograin size on the sensing abilities of CuO-SnO_2 composite nanofibers towards H_2S gas. The CuO-SnO_2 composite nanofibers were prepared by a sol-gel based electrospinning process. The nanograin size in CuO-SnO_2 composite nanofibers was changed by

calcination for different time intervals under the isothermal condition. The CuO-SnO_2 composite nanofibers with small-sized nanograins were highly sensitive towards H_2S gas compared to those comprised of larger nanograins. The stronger response of the CuO-SnO_2 composite nanofibers was explained based on the number of *p*-*n* junctions between the *p*-CuO and *n*-SnO_2 nanograins and higher resistance modulation during the transformation of *p*-CuO-*n*-SnO_2 to *metallic*-CuS-*n*-SnO_2 in the presence of H_2S and vice versa. The results show that optimization of the nanograin size is a vital parameter for achieving superior sensing properties and can be controlled by changing the calcination temperature and time.

Conflict of Interests

The authors declare that there is no conflict of interests regarding the publication of this paper.

Acknowledgment

This study was supported by Inha University Grant.

References

[1] C. H. Selene and J. Chou, "Hydrogen sulfide: human health aspects," in *Concise International Chemical Assessment Document*, WHO, 2003.

[2] J. Tamaki, K. Shimanoe, Y. Yamada, Y. Yamamoto, N. Miura, and N. Yamazoe, "Dilute hydrogen sulfide sensing properties of CuO-SnO_2 thin film prepared by low-pressure evaporation method," *Sensors and Actuators B: Chemical*, vol. B49, no. 1-2, pp. 121–125, 1998.

[3] C. Jin, H. Kim, S. An, and C. Lee, "Highly sensitive H_2S gas sensors based on CuO-coated $ZnSnO_3$ nanorods synthesized by thermal evaporation," *Ceramics International*, vol. 38, no. 7, pp. 5973–5978, 2012.

[4] R. B. Vasiliev, M. N. Rumyantseva, N. V. Yakovlev, and A. M. Gaskov, "CuO/SnO_2 thin film heterostructures as chemical sensors to H_2S," *Sensors and Actuators, B: Chemical*, vol. 50, no. 3, pp. 186–193, 1998.

[5] J. Kim, W. Kim, and K. Yong, "CuO/ZnO heterostructured nanorods: photochemical synthesis and the mechanism of H_2S gas sensing," *The Journal of Physical Chemistry C*, vol. 116, no. 29, pp. 15682–15691, 2012.

[6] G.-J. Sun, S.-W. Choi, A. Katoch, P. Wu, and S. S. Kim, "Bi-functional mechanism of H_2S detection using CuO-SnO_2 nanowires," *Journal of Materials Chemistry C*, vol. 1, no. 35, pp. 5454–5462, 2013.

[7] N. S. Ramgir, C. P. Goyal, P. K. Sharma et al., "Selective H_2S sensing characteristics of CuO modified WO_3 thin films," *Sensors and Actuators B: Chemical*, vol. 188, pp. 525–532, 2013.

[8] S. Park, J. Jung, T. Hong, S. Lee, H. W. Kim, and C. Lee, "H_2S gas sensing properties of CuO-functionalized WO_3 nanowires," *Ceramics International*, vol. 40, no. 7, pp. 11051–11056, 2014.

[9] A. Ebrahimi, A. Pirouz, Y. Abdi, S. Azimi, and S. Mohajerzadeh, "Selective deposition of CuO/SnO_2 sol-gel on porous SiO_2 suitable for the fabrication of MEMS-based H_2S sensors," *Sensors and Actuators, B: Chemical*, vol. 173, pp. 802–810, 2012.

[10] Y. Zhao, X. He, J. Li, X. Gao, and J. Jia, "Porous CuO/SnO_2 composite nanofibers fabricated by electrospinning and their H_2S sensing properties," *Sensors and Actuators B: Chemical*, vol. 165, no. 1, pp. 82–87, 2012.

[11] S.-W. Choi, J. Zhang, K. Akash, and S. S. Kim, "H_2S sensing performance of electrospun CuO-loaded SnO_2 nanofibers," *Sensors and Actuators B: Chemical*, vol. 169, pp. 54–60, 2012.

[12] S.-W. Choi, A. Katoch, J. Zhang, and S. S. Kim, "Electrospun nanofibers of CuO-SnO_2 nanocomposite as semiconductor gas sensors for H_2S detection," *Sensors and Actuators, B: Chemical*, vol. 176, pp. 585–591, 2013.

[13] J. Y. Park and S. S. Kim, "Growth of nanograins in electrospun ZnO nanofibers," *Journal of the American Ceramic Society*, vol. 92, no. 8, pp. 1691–1694, 2009.

[14] S.-W. Choi, J. Y. Park, and S. S. Kim, "Growth behavior and sensing properties of nanograins in CuO nanofibers," *Chemical Engineering Journal*, vol. 172, no. 1, pp. 550–556, 2011.

[15] J. Y. Park, K. Asokan, S.-W. Choi, and S. S. Kim, "Growth kinetics of nanograins in SnO_2 fibers and size dependent sensing properties," *Sensors and Actuators B: Chemical*, vol. 152, no. 2, pp. 254–260, 2011.

[16] A. Katoch, G.-J. Sun, S.-W. Choi, J.-H. Byun, and S. S. Kim, "Competitive influence of grain size and crystallinity on gas sensing performances of ZnO nanofibers," *Sensors and Actuators, B: Chemical*, vol. 185, pp. 411–416, 2013.

[17] J. Y. Park, S.-W. Choi, K. Asokan, and S. S. Kim, "Controlling the size of nanograins in TiO_2 nanofibers," *Metals and Materials International*, vol. 16, no. 5, pp. 785–788, 2010.

[18] R. Viter, A. Katoch, and S. S. Kim, "Grain size dependent bandgap shift of SnO_2 nanofibers," *Metals and Materials International*, vol. 20, no. 1, pp. 163–167, 2014.

[19] A. Katoch, S.-W. Choi, and S. S. Kim, "Nanograins in electrospun oxide nanofibers," *Metals and Materials International*, vol. 20, no. 2, pp. 213–221, 2015.